Si-H Bond Induced in H^+ Ion Implanted Silicon

N. Pradhan[1], S. Hajirnis[2], T. Thakur[3], N. Mhatre[4], L. Tribedi[5]

[1,2,3,4] Department of Physics, Ramnarain Ruia Autonomous College, Mumbai -400 019, India

[5]Tata Institute of Fundamental Research Centre, Colaba, Mumbai – 400 005, India

Authors name:

1) **Dr. Nana Pradhan**
Associate Professor in Physics
Department of Physics,
Ramnarain Ruia Autonomous College,
Mumbai -400 019, India

2) **Sarthak Hajirnis,**
Student, Physics,
2/16, Sachin Society, Mithagar Road,
Mulund east, Mumbai- 400 081, India

3) **Tanmay Thakur**
Student, Physics,
101, H-13, Indraprasth CHS, Pratiksha Nagar Depot,
Pratiksha Nagar, Sion , Mumbai 400 022, India

4) **Nikhil Mhatre**
Student, Physics,
H. No. 500/023, Laxmi Narayan Niwas,
Gothivali, Opposite Municipal School,
Navi Mumbai, Ghansoli S.O.
Thane - 400 701, India

5) **Dr. Lokesh Tribedi**
Professor, Nuclear and Atomic Physics,
Accelerator Based Physics Laboratory,
Department of Nuclear and Atomic Physics,
Tata Institute fo Fundamental Research,
Homi Bhabha Road, Colaba, Mumbai- 400 005, India

ABSTRACT *In this paper, p-type silicon <100> orientation, thickness (300 µm) wafers were uniformly implanted with 70 keV and 140 keV H^+ ions for the fluences of 2.5 × 10^{16} ions cm^{-2} and 5 × 10^{15} ions cm^{-2} respectively using Electron Cyclotron Resonance based Ion Accelerator (ECRIA) facility at Tata Institute of Fundamental Research (TIFR) centre, Mumbai, India. The structural properties non-implanted and implanted silicon samples were characterized using Raman spectroscopy and X-ray diffraction techniques. XRD and Raman techniques showed the formation of Si-H bond in 70 keV H^+ implanted silicon sample at fluence 2.5 × 10^{15} ions cm^{-2} sample. The compressive strain observed for 140 keV H^+ ions implanted silicon sample for the fluence of 5 × 10^{16} ions cm^{-2}. FWHM, strain and dislocation found to be varying in non-implanted and implanted sample.*

Keywords: *Ion Implantation, H^+ ion, Silicon, XRD, Raman Spectra.*

Introduction

Silicon, element with wondrous properties has proved to be most useful in technological advances in recent times. Use of Silicon can be found in many electronic devices due to its semiconducting properties. The presence of band gap between valence band and conduction band is useful in making Silicon work as transistors which in turn could be used as an amplifier or a switch. The properties such as bandgap, electron mobility, etc can be manipulated by introducing some defects in Silicon. Defects in Si can be of the form of doped elements, porosities, interstitial bonding of impurities with crystal, damaging the lattice structure, etc. Its advantages has benefited us so much that Porous Silicon has variety of applications such as gas sensors [1], solar cells [2-3], Bragg reflectors [4], photo catalysis [5]. The defects in Si can be

introduced in variety of ways; hydrogenation of Si has been a topic of research for many decades. The ability to passivate the electrical activity of dangling or defective bonds and deep defect impurity states in elemental and compound semiconductors has been of great interest for researchers [6-8]. By controlling the barrier height with shallow dopant implants, H^+ implants can be used to improve the characteristics of Schottky diodes [9]. Quantitative analysis of hydrogen in silicon is possible with accuracies better than 8% in total in hydrogen depth profiling [10]. Hydrogenation of Si can produce extended structural defects appearing as platelets with <111> orientation [11] and these defects correspond to high concentrations of hydrogen or deuterium as determined by various characterization techniques [12]. Surface hall mobility of silicon increases due to hydrogenation of silicon which can be used to increase the speed of IC [13]. Hydrogenation process can be carried out by ion-implantation. This process is highly suitable for making high-quality SOI wafers with the great advantages, related to the intrinsic properties of light ion implantation, of low defect density and thickness homogeneity [14].Though the implantation of hydrogen into Si has many advantages and substantially linear with fluence, small non-linear phenomena are observed, as revealed by few characterization processes [15]. Within a certain dose range, H implantation in Si forms platelets on two sets of habit planes, namely (001) and (111). At higher doses bubbles generally form instead of platelets [16].

In this paper, silicon samples were uniformly implanted using ion-implantation at moderate energy and different fluences. The structural properties of non-implanted and implanted samples were studied using Raman spectroscopy and X-Ray diffraction techniques.

Experimental Details:

Boron diffused silicon <100> wafers of thickness 300±20 μm and resistivity 5-10 Ω were procured from prolyx microelectronics. The samples were cut into 1×1 cm^2 dimension and cleaned using acetone after dissolving in the solution for two minutes. The cleaned samples were dried using UV lamp and allowed for ion implantation. The silicon sample were implanted with 70 keV H^+ ions for the fluence of 2.5×10^{16} ions cm^{-2} denoted as 'A' at ion depth 6264 Å, Whereas, the sample implanted with 140 keV H^+ ions for the fluence 5×10^{15} is denoted as 'B' having an ion depth of 1.23 μm . The ion energy depth profile was estimated using SRIM 2013 [17]. The pressure, ion current and deck temperature during implantation was maintained at 2×10^{-2} mbar, 2.5 - 4 μA and 18.4 ^{0}C respectively. The H^+ ion implantation was carried out at using Electron Cyclotron Resonance based Ion Accelerator (ECRIA) facility at Tata Institute of Fundamental Research (TIFR) centre, Mumbai [18] [19] .The non-implanted and implanted samples were characterized using Raman spectroscopy and XRD techniques. The Raman characterization was performed on EnSpectr R532 table top model on the samples. Raman spectra were characterized in the range 0-6000 cm^{-1}. XRD analysis was carried out using Rigaku 600 Miniflex machine (λ = 1.54 Å) at IR-Technology services at the range 10-110 degrees.

Results and Discussion

Raman Studies:

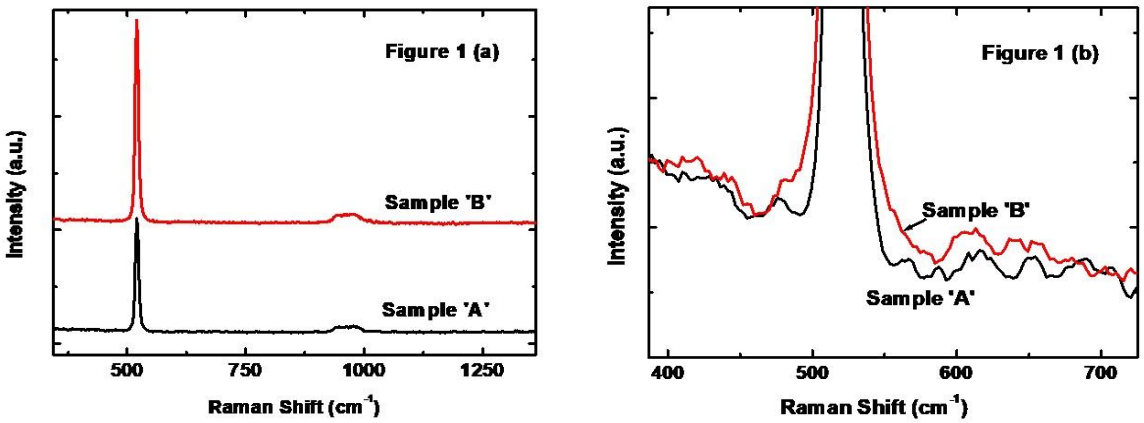

Figure 1: Raman spectra for silicon samples A and B in the ranges; (a) 450-1500 and (b) 400-700 cm^{-1}.

Figure1 (a) and 1(b) shows the Raman spectra of Sample A and Sample B in the range of 450-1500 cm^{-1} and 400-700 cm^{-1} respectively. It is observed that the silicon sample implanted with 70 keV showed the peak at 520.10 cm^{-1} attributed to the phononic silicon mode [Fig.1 (a)] with an intensity of 4161.36 cpf (counts per frame) and the shift in the peak with respect to non-implanted silicon($\Delta\upsilon = 0.40$ cm^{-1}) is found to the left for the 70 keV sample. However, Non-implanted p-type doped silicon sample shows its characteristic Raman mode at 520.5 cm^{-1} with an intensity of 1506.66 cpf. The result revealed that the shift in the sample is due to tensile stress induced in the lattice of Si-Si phononic mode [20]. The sample implanted with 140 keV showed the peak at 521.25 cm^{-1} which attributes to the silicon phononic mode [Fig.1 (a)] at the intensity of 7298.59 cpf and the right shift in the peak ($\Delta\upsilon = 0.75$ cm^{-1}) observed due to the increase in compressive stress in the Si lattice [20].

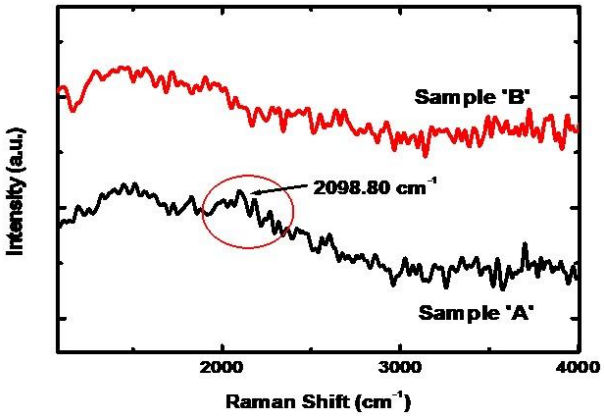

Figure 2: Raman Spectra of H^+ions implanted in Si for the sample A and sample B in the range of 1200 cm^{-2} to 4800 cm^{-2}.

Raman spectra of A and B samples plotted in the range of 1200 cm^{-1} to 4800 cm^{-1} as shown in Figure 2. The figure shows two different peaks at 1496 and 2098.80 cm^{-1}. The peaks observed at 1496 cm^{-1} and 2098.80 cm^{-1} confirmed the characteristics of silicon mode and attributes to the presence of hydrogen in Si lattice respectively [12]. This attributed peak of Si-H bond (2098.80 cm^{-1}) found to be weak with intensity 175.55 cpf. However, no prominent peak of Si-H bond is observed for the other sample [Fig 2]. This presence of H^+ ion in the silicon lattice cannot satisfactorily be confirmed as hydrogen storage device. Si-H bond having bond energy 3.296 eV (318 KJ/mol) and Si-Si bond having bond energy 2.301eV (222 KJ/mol) makes it difficult to harness the stored hydrogen without damaging the Si lattice; thus inefficient to use as a hydrogen storage. A significant change in the intensity of Raman spectra for hydrogen implanted samples is observed. Intensity is inversely proportional to fluence as with greater fluence. we also increase the prominent fluence so as to prepare the lower limit of amorphous substrate due to which the material enhances the properties. The distinguished peak observed at 479.6 cm^{-1} for sample 'A' [Fig, 1], which depicts a small degree of amorphous silicon formation [21]. The estimated FWHM found to be 8.92 cm^{-1} and 8.84 cm^{-1}at phononic mode for sample A and B respectively. The decrease in FWHM revealed the increase in crystallite size. Thus crystallite size for sample A is smaller than that of sample 'B' [22].

X-ray Diffraction (XRD) Studies:

Figure 3 shows XRD spectra of silicon samples at (a) non-implanted , (b) 70 keV H^+ implanted at the fluence of 2.5×10^{16} ions cm^{-2} (sample A) and (c) 140 keV at a fluence of 0.5×10^{16} ions cm^{-2} (sample B). XRD for the non-implanted sample showed peaks at 29.03 and 69.09 degrees attributed due to <111> and <100> reflections respectively [Fig.3(a)]. After implantation, the intensity of these reflections found to be increased due to formation of crystalline structures. The FWHM of sample A found to be increased than that of non-implanted sample [Fig 3(b)]. Whereas, FWHM of sample B is found to be decreased [Fig 3 (c)]. The estimated FWHM and crystallite size of non-implanted and implanted silicon sample showed in Table-I.

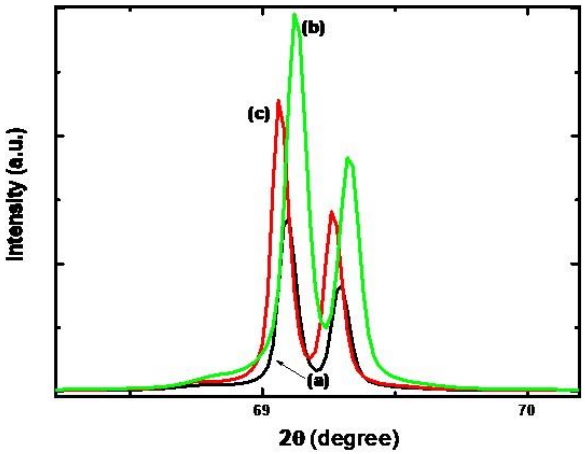

Figure 3: XRD spectra of; (a) non implanted and H^+ ions implanted silicon samples at: (b) 70 keV;2.5×10^{16} cm^{-2} and (c) 140 keV ; 0.5×10^{16} cm^{-2}.

The crystallite size of all samples estimated by the Scherrer's equation [23];

$$D = \frac{k\lambda}{\beta \cos\theta} \qquad (1)$$

Where D is the crystallite size, k is the Scherrer's constant which is set as 0.9, λ is the wavelength of X rays used, β is the full width half maxima along the plane (100) and θ is the Bragg angle. According to Williamson and Hall the broadening of diffraction lines is due to the contribution of crystallite size and strain of lattice [24]. The crystallite strain is given by,

$$\varepsilon = \frac{\beta}{4\tan\theta} \quad (2)$$

Where ε is the micro-strain of lattice, β is the FWHM of (100) plane and θ is the corresponding Bragg's angle. The strain in the sample A and B were found to be 32.0123 × 10^{-3} and 26.5954 × 10^{-3} respectively. However non-implanted sample showed the strain is 26.7743 × 10^{-3}. The variation in the strain in the implanted samples revealed that the deformation in the lattice of substrate.

The reduction in the crystallite size may be attributed to two aspects, one is large number bombardment of H^+ ions on crystal increases strain which is then more pronounced due to close packing of other crystals, and other is due to formation of strong Si-H covalent bond which pulls all the neighboring atoms of the lattice, thus reducing the lattice size.

The amount of defects in the sample is defined as the dislocation density [25] and is given by the equation;

$$\delta = \frac{1}{D^2} \quad (3)$$

The estimated dislocation density for the sample A and B is 274.747 × 10^{-3} and 189.332 × 10^{-3} nm^{-2}, whereas non-implanted sample showed 191.996 × 10^{-3} nm^{-2}.

It is evident that for higher ion fluence, higher is the extent to which dislocation takes place. These deformations give rise to observed changes in the physical parameters such as strain. At the higher fluence, probability of shifting silicon atom either in the interstitial space or displacing silicon atom and formation of Si-H bond takes place in the substrate material. The same result is revealed in the Raman study.

Table-I: XRD estimated data of FWHM and crystallite size of silicon samples

Sample	2θ (degree)	Intensity (a.u.)	β_{hkl} (degree)	Crystallite Size D (nm)
Non-implanted	69.09	5.31 × 10^5	0.07373	2.2822
A	69.13	1.11 × 10^6	0.08822	1.9078
B	69.07	8.73 × 10^5	0.07321	2.2982

Conclusion:

In this study hydrogen implanted silicon where characterized using Raman and XRD techniques. Raman spectra showed amorphous silicon at higher fluence. XRD spectra showed that changes in structural properties found to be more pronounced when implantation is carried out with high fluences. The structural studies revealed the formation of Si-H bond for the sample 70 keV at fluence 2.5 × 10^{15} ions cm^{-2}. Ion-implantation fluence plays a major role in producing defects. The lattice undergoes compressive stress when H^+ ions were implanted with energy of 140 keV and fluence of 5 × 10^{16} ions cm^{-2}. Whereas, the lattice undergoes the tensile stress when H^+ ions are implanted with energy of 70 KeV and fluence as high as 2.5 × 10^{16} ions cm^{-2}. Physical properties such as crystallite size, lattice strain and dislocation density is found to be varying with fluences and energies.

Acknowledgement:

The authors would like to thank K.V. Thulasiram for providing Electron Cyclotron Resonance based Ion Accelerator (ECRIA) facility at Tata Institute of Fundamental Research (TIFR) Centre, Mumbai, India.

References:

[1] Wei Yulong, Hu Ming, Yan Wenjun, Wang Dengfeng, Yuan Lin, Qin Yuxiang, 'Hydrothermal synthesis porous silicon/tungsten oxide nanorods composites and their gassensing properties to NO2 at room temperature', Appl. Surf. Sci., 353: 79, (2015).

[2] Asmiet Ramizy, Wisam J. Aziz, Z. Hassan, Khalid Omar, K. Ibrahim, 'Improved performance of solar cell based on porous silicon surfaces', Optik - International Journal for Light and Electron Optics, Vol. 122, Issue 23, (2011).

[3] Khaldun A. Salman, Z. Hassan, Khalid Omar, 'Effect of Silicon Porosity on Solar Cell Efficiency', Int. J. Electrochem. Sci., 7 , 376 – 386, (2012).

[4] VS Vendamani, ZY Dang, P Ramana, AP Pathak, VV Ravi Kanth Kumar, MBH Breese, et al. 'Fabrication of porous silicon based tunable distributed Bragg reflectors by anodic etching of irradiated silicon', Nucl.Instrum. Methods Phys. Res. Sect. B , 358: 105, (2015).

[5] Qu Yongquan, Zhong Xing, Li Yujing, Liao Lei, Huang Yu, DuanXiangfeng. 'Photocatalytic properties of Porous Silicon nanowires', J. Mater. Chem., 20, 3590, 22190767, (2010).

[6] A. J. R. DeKock, S.D. Ferris, L. C. Kimerling, H. J. Leamy, 'Investigation of defects and striations in as-grown Si crystals by SEM using Schottky diodes', Appl. Phys. Lett., 27, 313, (1975).

[7] S. J. Pearton, Murray Hill, J. W. Corbett, T. S. Shi, 'Hydrogen in Crystalline Semiconductors', Appl. Phys. A 43, 153-195, (1987).

[8] J. R. Weber, A. Janotti, P. Rinke, and C. G. Van de Walle, 'Dangling-bond defects and hydrogen passivation in germanium', Appl. Phys. Lett., 91, 142101, (2007).

[9] R. Singh and S. Ashok, 'Low energy hydrogen ion implantation in Schottky barrier control', Applied Physics Letters, 47, 426, (1985).

[10] J. F. Ziegler, C. P. Wu, P. Williams, C. W. White, B. Terreault, B. M. U. Scherzer, 'Profiling hydrogen in materials using ion beams', nuclear instruments and methods', 149, 19-39, (1987).

[11] S. Muto, S. Takeda & M. Hirata, 'Hydrogen-induced platelets in silicon studied by transmission electron microscopy', Philosophical magazine A, 72, 4, 1057-1074, (1995).
[12] N. M. Johnson, F. A. Ponce, R. A. Street, R. J. Nemanich, 'Defects in single-crystal silicon induced by hydrogenation', Phys. Rev. B, 35(8), 4166-4169, (1987)
[13] LI Jianming, 'Novel Semiconductor Substrate formed by Hydrogen ion implantation into Silicon', Chinese Phys. Lett. Vol.6, No.10, 458, (1989).
[14] H. J. Woo , H. W. Choi, G. D. Kim, J. K. Kim, W. Hong, Y. Y. Ji, W. B. Choi, Y. H. Bae, 'Application of hydrogen ion beams for soi wafer formation', Proceedings of APAC 2004, Gyeongju, Korea, (2004)
[15] G. f. Cerofolini , L. Meda, C. Volpones, R. Dierckx, G. Mercurio , M. Anderle, R. Canteri, F. Cembali, R. Fabbri and M. Servidori, 'Nonlinear phenomena in hydrogen implantation into (100) silicon', Nuclear Instruments and Methods in Physics Research Section B, Vol. 39, Issue 1-4, p. 26-29, (1989).
[16] S. Romani and J. H. Evans, 'Platelet defects in hydrogen implanted silicon', Nuclear Instruments and Methods in Physics Research B, 44, 313-317, (1990).
[17] J. F. Ziegler, M. D. Ziegler, and J. P. Biersack, Nucl. Instrum. Methods Phys. Res. B 268, 1818–1823 (2010).
[18] A. N. Agnihotri, A. H. Kelkar, S. Kasthurirangan, K. V. Thulasiram, C. A. Desai, W. A. Fernandez and L. C. Tribedi, 'An ECR ion source-based low-energy ion accelerator: development and performance', Phys. Scr. T144, 014038 (4pp), (2011).
[19] Shehla, A. Mandal, Ajay Kumar, M. Roy Chowdhury, Sanjiv Puri and L.C. Tribedi, 'Low-energy proton induced M X-Ray production cross sections for 70Yb, 81Tl and 82Pb', Nucl. Instr. Meth. Phys. Res. B 426, 34 (2018).
[20] Ingrid De Wolf, 'Stress Measurements in Si Microelectronics Devices using Raman Spectroscopy', J. Raman Spectrosc., 30, 877–883, (1999).
[21] X. Huang, F. Ninio, and L.J. Brown, S. Prawer, 'Raman scattering studies of surface modification in 1.5 MeV Si-implanted silicon', J. Appl. Phys., 77(11),(1995).
[22] C. Smita, R. A. C. M. M. van Swaaij, H. Donker, A. M. H. N. Petit, W. M. M. Kessels and M. C. M. van de Sanden, 'Determining the material structure of microcrystalline silicon from Raman spectra', Journal of Applied Physics 94, 3582, (2003)
[23] A. L. Patterson, 'The Scherrer Formula for X-Ray Particle Size Determination', Phys. Rev. 56, 978, Published 15 November (1939).
[24] P. Bindu, Sabu Thomas, 'Estimation of lattice strain in ZnO nanoparticles: X-ray peak profile analysis', J. Theor. Appl. Phys., 8, 123–134, (2014).
[25] Saleem, M., Fang, L., Ruan H. B., Wu, F., Huang, Q. L., Xu, C. L., Kong, C. Y., 'Effect of zinc acetate concentration on the structural and optical properties of ZnO thin films deposited by sol-gel method', Intl. J. Phy. Sci., 7(23), 2971–2979, (2012).